JEE Journal of Ecological Engineering

Journal of Ecological Engineering, 2025, 26(4), 209–219
https://doi.org/10.12911/22998993/199820
ISSN 2299–8993, License CC-BY 4.0

Received: 2024.12.23
Accepted: 2025.01.31
Published: 2025.02.17

Sorption of tetracycline from contaminated water using magnesium-iron layered double hydroxide alginate beads prepared from *Schanginia aegyptica* and scrap iron

Zainab Yahya Al-Rubaie[1*], Ayad A.H Faisal[1]

[1] Department of Environmental Engineering, College of Engineering, University of Baghdad, Baghdad, Iraq
* Corresponding author's email: zainab.yahia2111p@coeng.uobaghdad.edu.iq

ABSTRACT

This research was conducted to produce a nonconventional sorbent with the aid of *Schanginia aegyptica* and scrap iron solid wastes. The solutions extracted from Schanginia plant parts and scrap iron can be used effectively to prepare magnesium and iron ions, respectively. The prepared sorbent named "magnesium / iron-layered double hydroxide-sodium alginate beads (Mg/Fe-LDH-Na alginate beads)" was studied to capture tetracycline (TC) from the wastewater based on batch study. The best conditions optimized to prepare the afore-mentioned beads were Mg/Fe molar ratio = 3, initial pH 10, and Mg/Fe-LDH dosage = 5 g per 100 mL. Langmuir and pseudo-second-order model adequately describe isotherm and kinetic sorption suggesting a maximal capacity of 2.564 mg/g and there are chemical bonds between TC and alginate beads. The bead characterization tests revealed the formation of Mg/Fe-LDH nanoparticles that are responsible for TC with the presence of functional groups like hydroxyl (OH) groups.

Keywords: tetracycline, adsorption, *Schanginia aegyptica*, sodium alginate, scrap iron.

INTRODUCTION

TC is a commonly applied antibiotic and, accordingly, it is detected in various water resources (Dai et al., 2020). Eliminating TC from the water and wastewater is considered a complex task that needs practical and scientific efforts. Adsorption plays a vital role for treating solutions containing TC because of its efficiency, easy operation, low cost, and regeneration (Majeed et al., 2017; Ahmed et al., 2020).

The sorbent selection is considered a major operative point; especially, such materials should be efficient, inexpensive, stable, and eco-friendly. Several sorbents were utilized in the previous studies for removing TC from solutions including activated carbon, zeolite, clay, chitosan, and montmorillonite (Ali, 2015; Ebrahim and Alhares, 2015; Elmoubarki et al., 2015; Salman et al., 2023). However, low sorption capacity, high cost and poor reuse rate are considered the main disadvantages of these sorbents which limits their utilization. Thus, the development of an innovative sorbents that avoid such limitations can be considered a vital task. Therefore, nanoparticles are used to eliminate TC from wastewater due to tunable surface characteristics, high area of surfaces, and rapid sorption kinetics, making them highly efficient sorbents. Magnetic chitosan, graphene oxide, titanium dioxide and layered double hydroxides (LDHs) are examples for such materials (Alanazi et al., 2024; Sadegh et al., 2017).

LDHs are ionic compounds consisting of positively charged layers, such as the mineral brucite, with molecules between the structure of these layers at the center of the octahedra that have cations sharing edges, surrounded by OH^- ions (Moaty et al., 2019). Different LDHs were manufactured and used as sorbents to remove TC from wastewater. In this regard, co-precipitation was used to prepare the sorbent of core-shell Fe_3O_4-LDHs and investigate its properties upon adsorption. There are different synthesis methods of preparing such materials like co-precipitation

(Greenwell et al., 2010), hydrothermal methods (Tonelli et al., 2021), and microwave irradiation (Kameliya et al., 2023).

Green synthesis methods were used for preparing LDHs. These methods minimize the environmental impact while enhancing the functionality and applicability of LDH including the use of plant-based reducing agents, hydrothermal synthesis with organic compounds, and eco-friendly co-precipitation (Osman et al., 2024). The extraction of metals from waste or plants for the synthesis of LDHs is a forward-thinking strategy that promotes both environmental conservation and economic efficiency by waste management, reducing volume the need for landfills, and cutting down on the toxic chemicals and energy (Kiani et al., 2022; Osman et al., 2024); this procedure is known as "green synthesis".

Schanginia (SC) considers a type of plants that available in huge quantities through the environment of Iraq and regions with arid climate. SC is a manganese-rich plant and contains flavonoids, alkaloids, saponins, tannins, and glycosides (Yaseen et al., 2022). Therefore, the wastes of this plant can be used to be the source for magnesium ions. Also, huge amounts of scrap iron are produced every day in certain industrial workshops in Baghdad, Iraq. Statistical survey among 11 workshops revealed that a total production of 13.2 tons of raw scrap for each day is equivalent to 1.2 tons scrap iron per workshop (Rashid and Faisal, 2018). These large waste quantities could be utilized as source for iron to prepare LDH in combination with Mg from SC. Accordingly, preparation and characterization of Mg/Fe LDH alginate beads from the Schanginia and iron scrap solid wastes were the focal aspect of this work. The efficacy of the prepared beads was evaluated in terms of the TC antibiotic elimination from aqueous solution.

EXPERIMENTAL WORK

Materials and methods

High-purity chemicals, such as HCl (hydrochloric acid), NaOH (sodium hydroxide), $CaCl_2$ (chloride of calcium), and $NaC_6H_7O_6$ (sodium alginate with 2.5×10^5 g/mol, obtained from Sigma Aldrich, USA) were utilized. TC was chosen as a model contaminant for simulating water contamination. Contaminated water was prepared by dissolving TC ($C_{22}H_{24}N_2O_8$, from Samarra Drugs Factory) in water to prepare 1000 mg/L stock solution, which was then used for batch tests. The water pH can be adjusted by adding 0.1 M NaOH or HCl as needed. TC concentration can be measured using UV-visible spectroscopy (UVmini-1240, Shimadzu, Japan).

Preparing of Mg/Fe-alginate beads

The core of this study involved the extraction of magnesium and iron from Schanginia (SC) and iron scrap, respectively, which are abundant in the environment, followed by their immobilization in sodium alginate beads. The preparation process consisted of several steps:

1. Schanginia waste (stem, leaves, and fruits) was collected from Madhatiya, Babylon Governorate, dried under the sun, and then dried at 85 °C using oven to remove moisture. The dried plant had to be ground and passed through 20-mesh sieve. It was then soaked, washed, and dried at 105 °C before being ground into powder. Iron scrap was obtained from blacksmiths in Hillah city.
2. For extracting the highest concentrations of magnesium and iron, different quantities of SC or iron scrap powder (3, 5, 10, 15, and 20 g) and various concentrations of hydrochloric acid solution (2, 4, 10, and 14%) were tested under agitation for 3 hours at 20 °C. The resulting solutions were passed through filter papers to separate the solid particles from the magnesium or iron ions.
3. Two solutions containing magnesium and iron ions were mixed in Mg/Fe ratios (0.5, 1, 2, 3, 4, and 5) and subjected to precipitation by adjusting the pH using 1 M NaOH to find the best pH (7, 8, 9, 10, 11, and 12). The mixture was stirred until precipitates formed, which were separated, dried at 85 °C, rinsed with DW (distilled water), annealed at 200 °C for 8 h, and ground into powder.
4. The 2 g Na-alginate was dissolved in 100 mL DW and agitated for 24 hours to produce sodium alginate solution. Various amounts of nanoparticles werre added to the produced solution, and the slurry had to be inserted into 0.1 M $CaCl_2$ to form beads. The beads were dried at 105 °C. The preparation steps are illustrated in Fig. 1, and the effectiveness of the prepared beads for TC removal was used to determine the optimal conditions for synthesis.

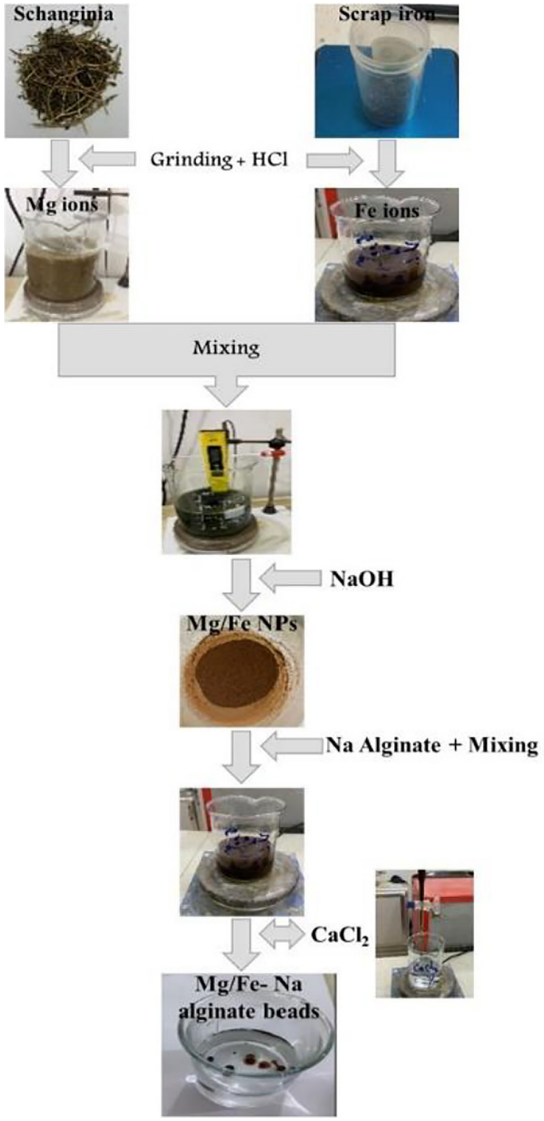

Figure 1. Experimental procedure for synthesis of Mg/Fe LDH - sodium alginate beads

Batch study

By batch experiments, the kinetic and equilibrium of TC capture onto prepared beads were implemented. The experiments were arranged to distinguish the suitable contact time, initial pH, agitation speed, and the amount of beads required to capture the most TC molecules at specific C_o. A number of flasks are prepared and a certain volume of simulated polluted water (V = 100 mL) had to be poured into each flask. Specific mass of prepared beads (m) was combined with polluted water within the flasks and the flask were agitated for 3 h at 250 rpm. At the end of agitation, the beads were isolated by filter paper, and equilibrium TC concentration (C_e) was evaluated by UV-visible spectroscopy. The mass of TC captured in the prepared beads at the equilibrium (q_e) can be calculated from Equation 1 (Wang and Wang, 2015).

$$q_e = (C_o - C_e)\frac{V}{m} \quad (1)$$

MODELING OF SORPTION DATA

The familiar models apply to formulate the equilibrium sorption measurements and finding the behavior of sorbents as well as its sorption capacity are Freundlich and Langmuir models (Table 1). On the other hand, the pseudo-first order and pseudo-second order models are popular relationships applied to understand the kinetic of contaminant removal (Qiu et al., 2009).

RESULTS AND DISCUSSION

Extraction Mg ions from Schanginia

The SC was used as the source of Mg ions; however, many elemental ions like Fe, Mn, and Zn were measured in the extracted solution. Fig. 2 explains the concentrations of these ions that can be extracted from SC under the variation of HCl concentrations (2–14%) and dosages of SC (10–140 g/300 mL). Results indicate that the increasing of HCl generally lead to higher yields of extracted Fe,

Table 1. Equilibrium and kinetic models applied for formulation of sorption results

Model	Equation	Parameter	Reference
Freundlich isotherm	$q_e = K_f C_e^{1/n}$	q_e – equilibrium sorption capacity, K_f – Freundlich constant, n: sorption intensity	(Lucas et al.,2004)
Langmuir isotherm	$q_e = \frac{q_m b C_e}{1 + bC_e}$	q_m – maximum sorption capacity, b — affinity constant	(Lucas et al., 2004)
Pseudo-first order	$q_t = q_e(1 - e^{-k_1 t})$	k_1 – rate constant, q_t – solute quantity sorbed at time (t)	(Yagub et al., 2012)
Pseudo-second order	$q_t = \frac{t}{\left(\frac{1}{k_2 q_e^2} + \frac{t}{q_e}\right)}$	k_2 – rate constant	(McKay et al., 1999)
Intra-particle diffusion	$q_t = k_{int} t^{0.5} + C$	k_{int} – the sorption rate constant (mg/g min$^{0.5}$), C – the intercept	(Cheung et al., 2007)

Mn, and Zn metal ions. The Fe Mn, and Zn concentrations have maximum values of 287.4, 22.5, 21.4 mg/L, respectively, when the HCl concentration is equal to 14% for SC dosage 20 g/300 mL. The same figure shows that the highest concentration of Mg is equal to 7440.5 mg/L, occurring at 4% HCl and SC dosage 20 g/300 mL. This may be due to the metals in the SC material likely being bound in the form of insoluble metal oxides, hydroxides, carbonates, or other compounds; however, the present results are compatible with the findings of previous research (Sutherland and Tack, 2008). Figure 2 certifies that the highest concentration of extracted metal ions was Mg in comparison with other measured ions included Fe, Mn, and Zn; thus, the SC can be used to supply Mg ions. Addition of higher SC dosage can lead to decrease in the extracted Mg concentration and this can result from; increasing of viscosity and reducing of mass transfer rates, insufficient HCl available to fully solubilize the metals, and potential re-adsorption or precipitation of extracted metals (Sutherland and Tack, 2008; Ujaczki et al., 2017).

Extraction of Fe ions from iron scrap

The extraction of iron (Fe) from iron scrap was investigated by varying the concentration of HCl while keeping the dosage of iron scrap constant at 20 g per 300 mL. Figure 3(a) signifies that the Fe concentration varies from 40010 to 402097 mg/L as the HCl percentage changes from 2 to 14%; however, the highest concentration of Fe (410451 mg/L) occurred at 4% HCl. Also, the extraction of Fe was investigated by variation the iron scrap mass from 3 to 25 g per 300 mL for 4% HCl. Fig. 3(b) shows that the extraction efficiencies of Fe are increased with the iron scrap dosage up to a peak value (410451 mg/L), obtained at 20 g per 300 mL. This figure certifies that the using higher or lower value of 20 g per 300 mL can be associated with clear decrease in the extracted of Fe ions. Hence, the best extraction of Fe ions can be adopted with 4% HCl for iron scrap dosage of 20 g per 300 mL.

Synthesis of beads

The role of pH in the manufacture of Mg/Fe-LDH beads was investigated within (7–12) where Mg to Fe molar ration = 1 and LDH nanoparticles mass = 5 g per 100 mL. For tests of sorption, 0.5 g of beads was mixed with 50 mL solution, where C_o of antibiotic 10 mg/L, initial pH 7, agitation 250 rpm and contact time 3 hours. It is obvious from Fig. 4(a) that the sorption capacity of beads for TC was varied from 0.66 to 1.14 mg/g due

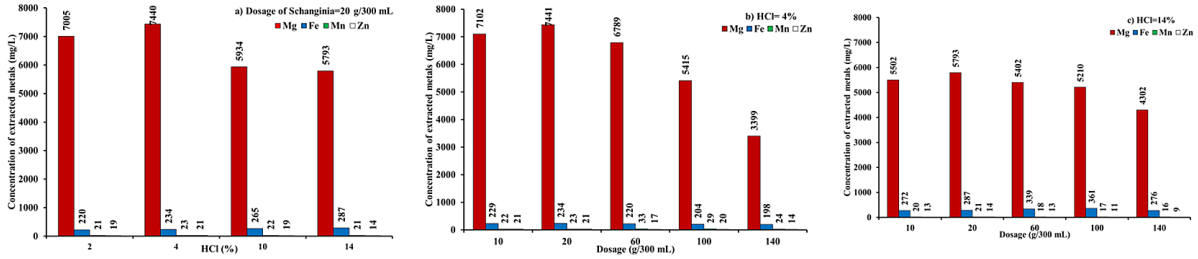

Figure 2. Effects of (a) dosage and (b & c) HCl percentage on the extraction of Mg, Fe, Mn, and Zn metal ions from Schanginia plant

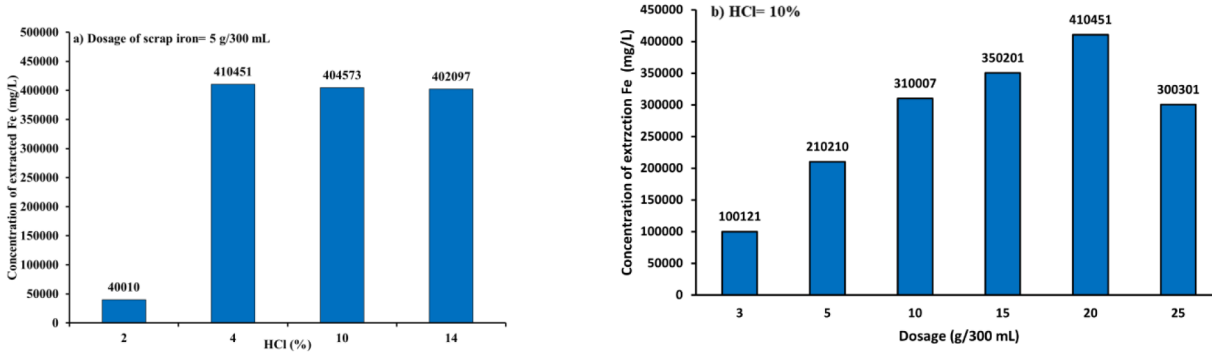

Figure 3. Effects of (a) HCl percentage and (b) dosage of scrap iron on the extraction of Fe metal ions

to the change of pH from 7 to 12, respectively. This figure explains that the pH=10 is suitable to achieve the highest adsorption capacity of TC (1.22 mg/g) from aqueous solution. The effect of different values of Mg/Fe ratio on the TC sorption capacity was examined. The sorption experiments are applied under the same operational conditions illustrated previously with pH and Mg/Fe LDH nanoparticles equal to 10 and 5 g/100 mL for synthesis. Figure 4(b) proves that the TC adsorption capacities were varied from 1.14 to 1.02 mg/g due to vary of Mg/Fe from 0.5 to 5, respectively. The results suggest that a molar ratio of 3 provides the highest TC adsorption capacity with value of 1.36 mg/g. The present study explored the TC adsorption capacities with Mg/Fe LDH nanoparticles dosage variation from 0.5 to 5 g/100 mL at pH 10 and Mg/Fe 3 using the operational conditions for sorption tests as mentioned previously (Fig. 4c). It is clear that the sorption capacity for TC increases from 1.14 to 1.542 mg/g identical to change of nanoparticle mass from 0.5 to 5 g/100 mL. Various materials and methods have been explored for the adsorption of TC; for instance, modified alginate beads demonstrated an adsorption capacity of 356.57 mg/g at pH 5 (Luo et al., 2021), while copper alginate beads achieved a higher capacity of 533 mg/g (Chen et al., 2022). Calcium/iron-layered double hydroxides (Ca/Fe-LDHs) in sodium alginate formed spherical particles with high adsorption efficiency (Abed and Faisal, 2023). The advantages of Mg/Fe-LDH alginate beads include their cost-effectiveness due to the use of scrap iron and natural alginate. However, they also present disadvantages, such as lower adsorption capacity compared to some other adsorbents, a limited effective pH range that necessitates maintaining optimal conditions, and potential concerns regarding the leaching of TC into treated water.

Sorption tests

The behavior of TC sorption efficiency for time up to 180 minute at pH 7, C_o 10 mg/L, sorbent mass 0.5 g/100 mL, and speed 250 rpm is represented by Figure 5(a). Till 120 min, the antibiotic is eliminated with high rate and; thereafter, it is greatly reduced due to the decrease in the binding sites. The TC sorption efficiency is 75% at 120 min and this percentage approximately stabilizes beyond this time till 180 min. This behavior is consistent with findings from other studies, such as those involving Al-Fe pillared clay, where optimal removal was also achieved at around 120 minutes, indicating that sufficient contact time is crucial for maximizing adsorption (Al-Kindi and Alnasrawy, 2022).

Figure 5(b) proves that the capture efficiency of TC is dependent on C_o. These efficiencies were significantly decreased from 81.4 to 23.5% due to change of C_o from 5 to 200 mg/L at 120 min, pH 7, dosage 0.5 g/100 mL and 250 rpm. All of the TC molecules are expected to engage with the accessible binding sites at lower concentration of contaminant, which will definitely lead to a significant increase in sorption efficiency (Park et al., 2002). This trend aligns with other research showing that lower initial concentrations lead to higher removal rates due to more available binding sites being utilized effectively (Al-Kindi and Alnasrawy, 2022). For instance, studies on calcium hydroxide-modified biochar reported similar results where higher concentrations resulted in reduced adsorption efficiency (Wang et al., 2023).

The impact of agitation speed on antibiotic removal efficiency is seen in Figure 5(c). It has been noted that removal efficiency can rise significantly with increased speed. Actually, the increased agitation speed promotes the diffusion

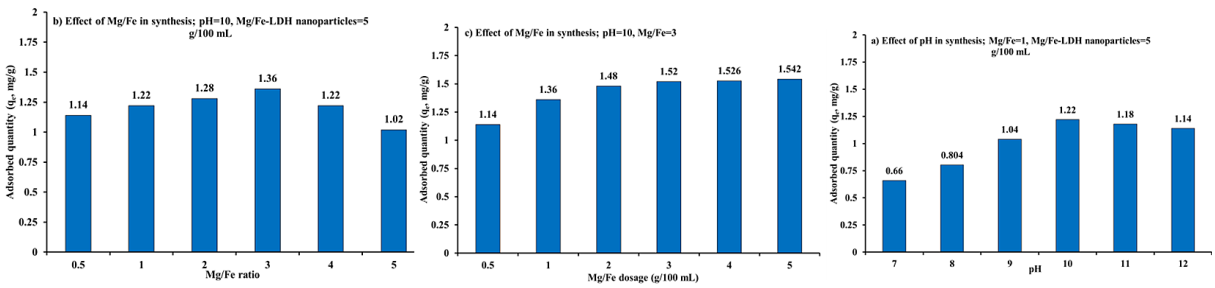

Figure 4. Effect of (a) pH, (c) Mg/Fe ration and (d) Mg/Fe-LDH dosage on the TC removal efficiency by prepared beads for sorption conditions (time=3 h, C_o=10 mg/L, sorbent dosage=0.5 g/50 mL, pH 7, speed 250 rpm)

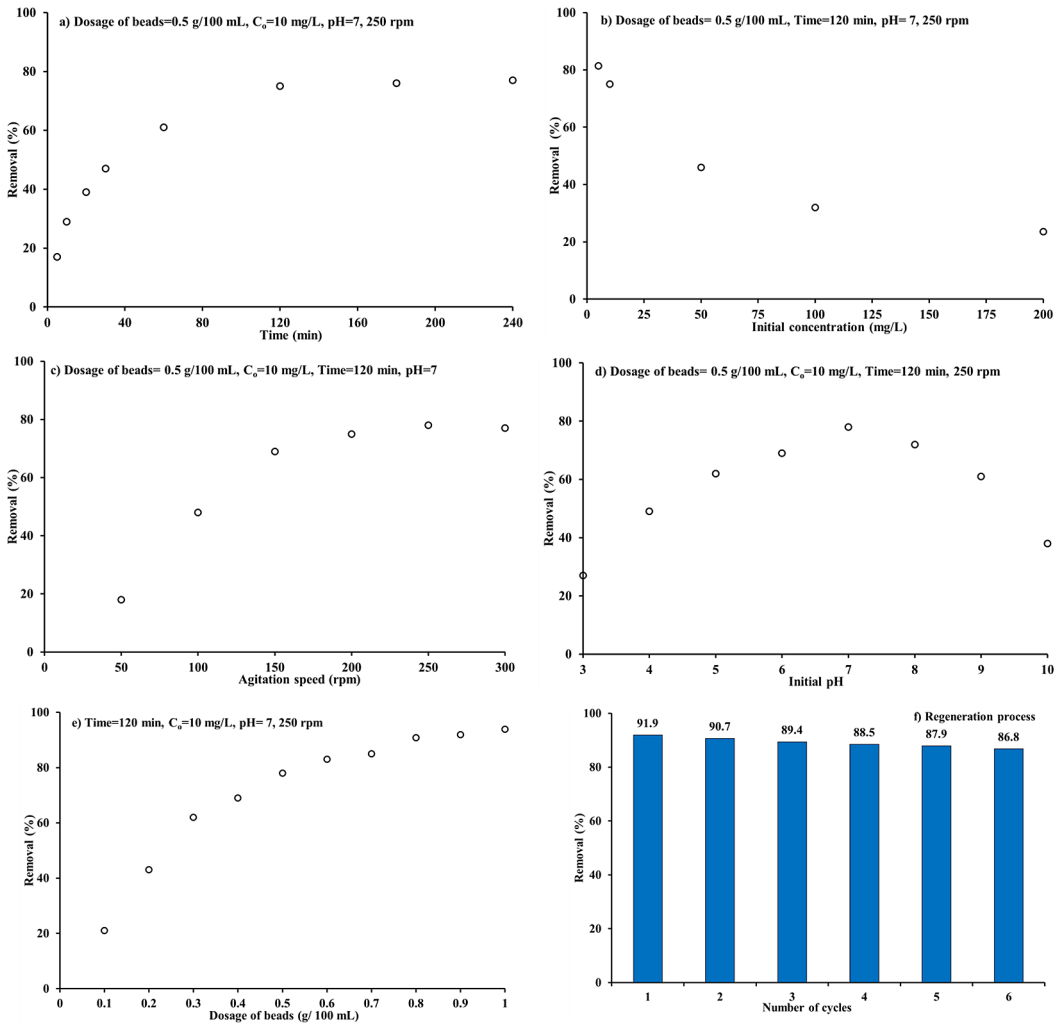

Figure 5. Effect of batch conditions on TC removal from aqueous solution by prepared beads at room temperature (a-e), as well as (f) the regeneration process for exhausted beads

of the antibiotic through the Mg/Fe LDH alginate beads, which makes it possible for the TC molecules and the accessible binding sites to form a suitable association. The speed of 250 rpm was found to be adequate to ensure maximum efficiency (78%), and there is no remarkable difference in the removed TC beyond this value, according to the measured data (Elkady et al., 2011) which is corroborated by findings from other studies that emphasize the importance of mixing in enhancing adsorption kinetics (Al-Kindi and Alnasrawy, 2022). In comparison, some biochar studies suggest that while agitation improves performance, the optimal speed may vary based on the specific adsorbent and its characteristics (Zhang et al., 2023).

The pH of an aqueous solution is another important consideration, since it greatly affects the removed TC. As shown in Figure 5(d), this calls for carrying out tests with stabilized other operational parameters and defined beginning pH ranges, specifically from 3 to 12. Up to a pH of 7, the elevation in pH clearly produced a notable improvement in the TC removal; after this point, the removal percentage fell. The reason for this behavior is as follows: at pH 3, the TC removal percentage was low (=27%) because the antibiotic and H^+ were competed for the sorption sites on the surface of the beads. As pH increased, the removal percentage also increased, reaching its maximum value (78%) at pH 7. Due to the hydrogen bonding-induced adsorption, TC exhibits reduced ionization and hydration in its neutral state. The sorption capacities of beads exhibit a tendency to decrease in response to a rise in pH, which slows down hydrogen bonding because OH ions are formed. This implies that when the antibiotic reacted with the oxygen (hydroxyl group) that was present on the bead surface, the sorption mechanism was complex (Asaoka et al., 2021).

This observation is supported by other research, for example, calcium hydroxide-modified corn straw biochar exhibited enhanced performance at neutral pH levels due to reduced ionization of tetracycline (Wang et al., 2023). Conversely, some materials like Al-Fe pillared clay showed optimal performance at lower pH values around 4.5 (Al-Kindi and Alnasrawy, 2022).

To determine the ideal dosage, the effects of sorbent g on the TC uptake were investigated for values from 0.1 to 1 g per 100 mL of the solution. Figure 5(e) indicates that as the mass of the beads increases, so may the effectiveness of TC removal. This is demonstrated by the fact that the effective regions increased with higher beads dosage (Ge et al., 2017). Due to change in bead mass from with mentioned range, the sorption effectiveness varied from 21 to 93.9%; 1 g/100 mL appears to be the optimal dosage. This trend aligns with findings from other studies where higher adsorbent dosages correlate. For instance, the research on Al-Fe pillared clay demonstrated a similar pattern where increasing adsorbent dosage led to higher tetracycline removal rates until a saturation point was reached (Al-Kindi and Alnasrawy, 2022). Mg/Fe LDH alginate beads have demonstrated 93.9% from water under optimal conditions: 1 g/100 mL, 120 min, 10 mg/L, pH 7, and 200 rpm. This performance is comparable to other adsorbents, such as chitosan-based magnetic adsorbents with a removal efficiency of 73.69% (da Silva Bruckmann et al., 2022), and copper alginate with removal 54.6% (Chen et al., 2022). These findings suggest that Mg/Fe LDH alginate beads are effective for tetracycline removal from water.

Reusability

The viability of reusing the spent beads for TC removal must be evaluated through cycles of adsorption and desorption. 0.5 M HCl is used in the regeneration process to desorb TC from used beads. The percentages of TC eliminated in response to the recycles number are displayed in Fig. 5(f), where it is evident how well beads are regenerated. Reusability is an important factor to evaluate the performance of beads and their suitability for real applications, because it can drastically lower operating costs and make the process affordable. Five consecutive rounds of the identical batch conditions were employed. The capacity of the reused beads can be around 89.4% at the conclusion of the third cycle, and the quantity of TC eliminated in the first cycle was 91.9%, as shown in Figure 5(f). When compared to other materials, Mg/Fe-LDH alginate beads exhibit competitive reusability characteristics. For example, studies on activated carbon have reported varying degrees of reusability depending on the regeneration method used; some activated carbons maintained efficiencies above 80% after three cycles (Singha et al., 2022). On the other hand, the leaching concentration of Mg^{2+} and Fe^{3+} from the Mg/Fe-LDH alginate beads results in the solution of 39.7 and 18.1 mg/L, respectively.

Characterization analyses

The XRD patterns of Mg/Fe LDH sodium alginate beads are shown in Figure 6(a), where the emergence of a new peak at 26.6° suggests the existence of Mg/Fe-LDH crystalline phases (Ahmed et al., 2020). It is obvious that the accurate manufacture of Mg/Fe-LDH beads was accomplished. In Figure 6(b), the FT-IR spectra of the produced beads after and before TC sorption are shown to identify the main functional groups that improved TC sorption. This figure demonstrated how stretching vibrations experienced by amides and (-OH) groups result in the creation of high intensity absorption bands. The stretching vibrations of hydrogen bonds and OH groups produced a prominent and broad absorption band at (3550–3200 cm^{-1}) in the peaks of alginate beads. Stretching vibrations of the OH and C-H are correlated with peaks at 3464 cm^{-1} (Faisal et al., 2020; Islam et al., 2016). The stretching vibrations of Fe-O (ferrite skeleton included) and Mg-O bonds corresponded to the absorption bands at 513 and 667 cm^{-1} (Ahmed et al., 2020). The SEM-EDS analysis was carried out to identify the morphological properties of prepared beads after and before loaded with TC. Figure 7(a) depicts the mean particle, indicating that the prepared beads surfaces have a nonhomogeneous morphology. However, at 10 μm magnification scales, the surface may be extremely compact and disordered. It appears that the beads have a micro-porous surface that enables oxyanions to be absorbed. Comparing to the beads prior to the sorption process, there are notable changes in the beads morphology after the TC sorption (Fig. 7(b)). The EDS test describes the change magnitude observed in the percentages of elements for the composition of alginate beads after the sorption process, as shown in Tables listed within Fig.

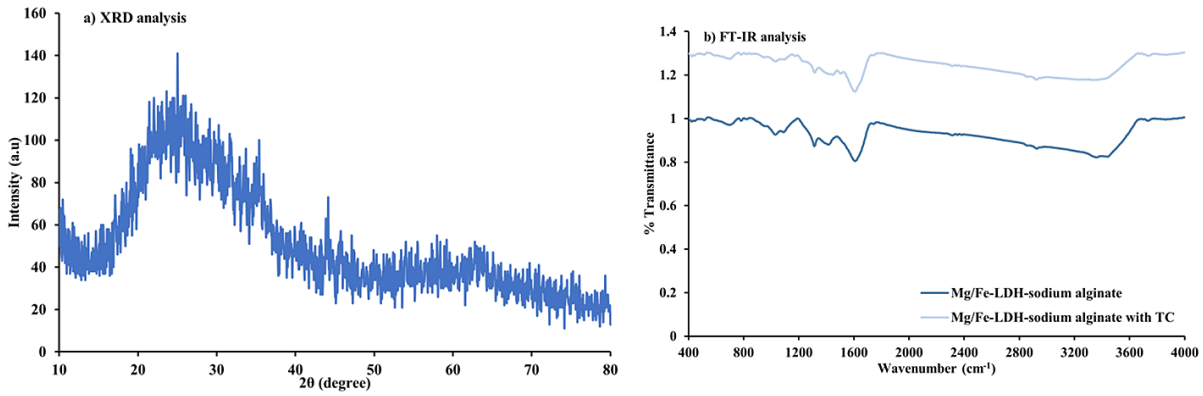

Figure 6. Characterization of prepared Mg/Fe-LDH alginate beads by a) XRD and b) FT-IR analyses

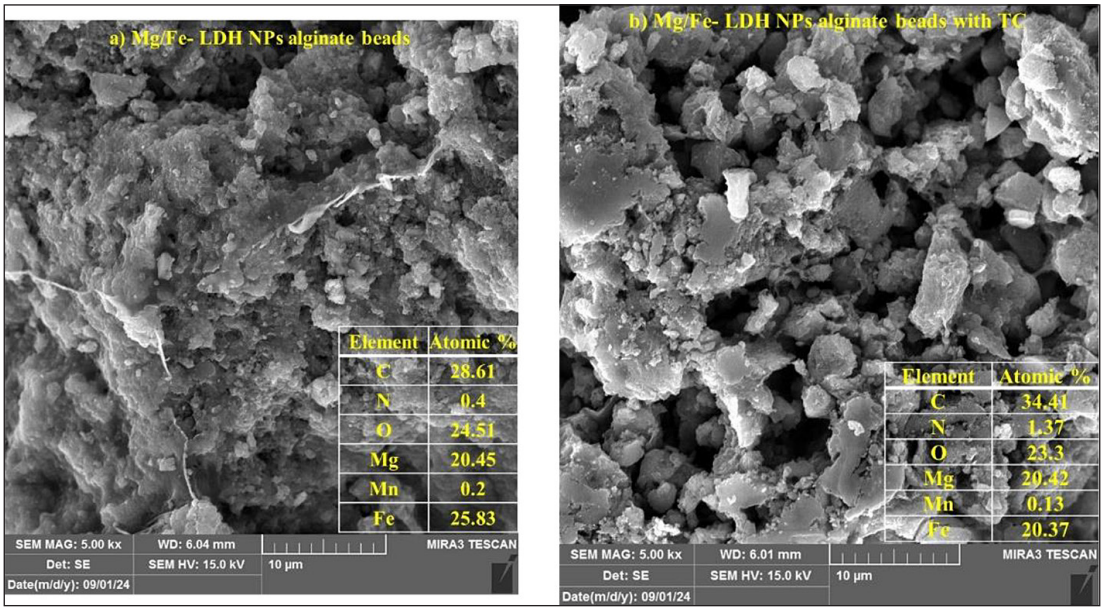

Figure 7. Morphological characteristics using SEM-EDS analysis for Mg/Fe- NPs sodium alginate beads (a) before and (b) after sorption of TC

7(a, b). These tables prove the presence an increment in C content after TC sorption.

Isotherm and kinetic of sorption measurements

The sorption isotherm models discussed earlier were utilized to interpret the sorption equilibrium outcomes due to TC interactions with the Mg/Fe LDH beads. Table 2 lists the parameters for Freundlich and Langmuir models obtained from fitting of these models with equilibrium sorption measurements as expressed in Figure 8(a) using nonlinear regression option in Microsoft Excel. This figure presents the models' performance against the experimental data. For Table 2 and Figure 8(a), it is evident

Table 2. Constants of isotherm and kinetic models with statistical measures for sorption of TC onto Mg/Fe-LDH-alginate beads

Model	Parameter	Value
Freundlich	K_f (mg/g) (L/mg)$^{1/n}$	1.175
	n	3.076
	R^2	0.912
Langmuir	q_{max} (mg/g)	2.564
	b (L/mg)	0.746
	R^2	0.947
Pseudo-first order	q_e (mg/g)	1.500
	k_1 (1/min)	0.036
	R^2, SSE	0.986, 0.041
Pseudo-second order	q_e (mg/g)	1.706
	k_2 (g/mg min)	0.026
	R^2, SSE	0.996, 0.010

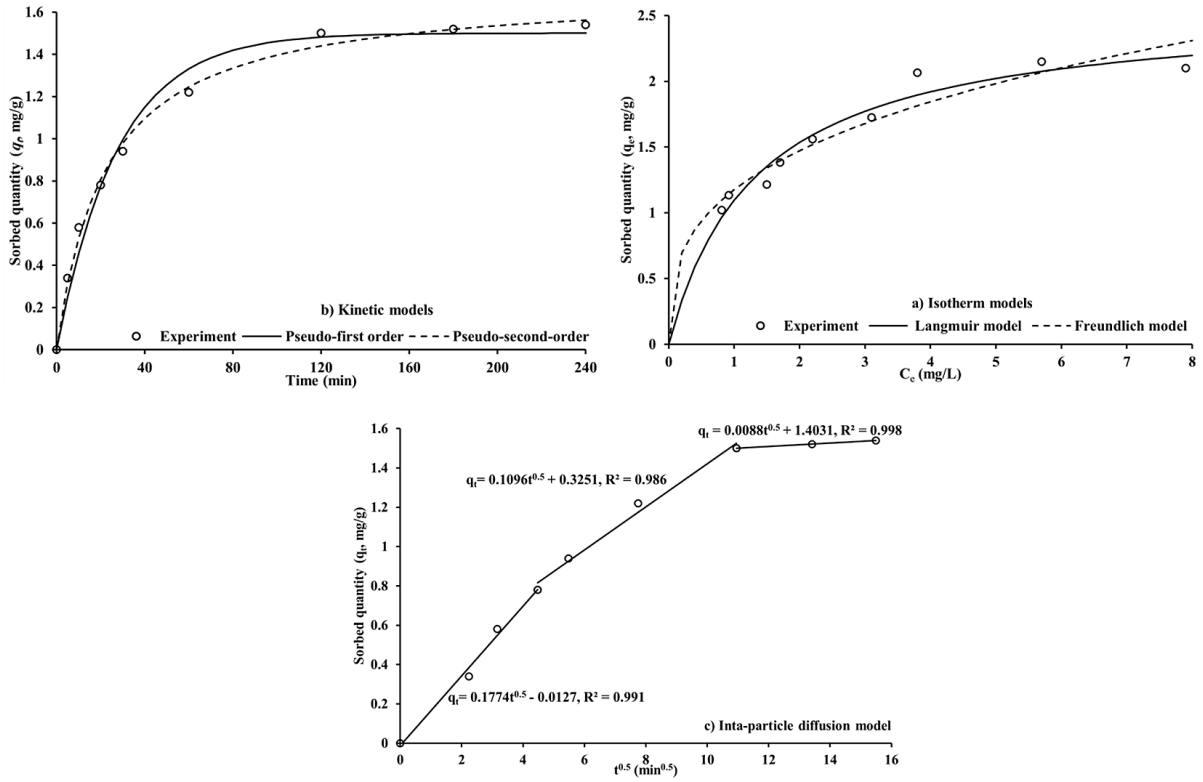

Figure 8. Formulation of sorption measurements using (a) isotherm models, (b) kinetic models, and (c) intra-particle diffusion model for interaction of Mg/Fe-LDH beads with water contained TC

that the Langmuir model exhibits a higher determination coefficient, R^2 in comparison to the Freundlich model, indicating a better fit and a more accurate representation of the sorption process. This suggests that the TC molecules sorbed primarily as a monolayer on the beads surface. The maximum sorption capacity has value of 2.564 mg/g as determined from the Langmuir model.

The sorption kinetics were formulated by pseudo-first-order and pseudo-second-order models, as illustrated in Figure 8(b). Table 2 lists the parameters of such models, including R^2 and sum of square errors (SSE). This table reveals that the TC sorption kinetics is more compatible with the second model, as indicated by the higher R^2 and lower SSE. This suggests that the chemical forces can be bonded of TC molecules with alginate beads.

The kinetic measurements were further studied by the intra-particle diffusion model (Table 1), revealing linear relationships between $t^{0.5}$ and q_t with acceptable R^2 values, as depicted in Figure 8(c). The intercepts of lines with y-axis indicate the occurrence of intra-particle diffusion, in spite of it not being the rate-controlling step. The observed deviation from the origin point suggests that diffusion limits the rate of sorption (Cheung et al., 2007).

CONCLUSIONS

The Mg and Fe ions were successfully extracted from Schanginia aegyptica and scrap iron, which were produced in large quantities as solid waste. In order to create Mg/Fe-LDH nanoparticles using the precipitation method, the ions must be mixed together. The creation of spherical beads requires immobilizing the produced nanoparticles with sodium alginate. Batch experiments were used to assess the ability of spherical beads to extract TC from aqueous solution. Nanoparticle mass of 5 g per 100 mL, pH 10 and (Mg/Fe) molar ratio = 3 are the ideal values for the production of beads. Langmuir and pseudo-second-order models are able to depict the sorption interaction with high capacity of 2.564 mg/g. The formation of magnesium/iron-LDH nanoparticles in the prepared beads was certified through characterization analyses; yet, the rise in the carbon percentages indicates the presence of TC sorption.

Acknowledgements

The authors would like to express their sincere gratitude to Baghdad University for its invaluable support and provision of resources that greatly facilitated the successful completion of this research.

REFERENCES

1. Abd Ali, Z. T. (2015). A comparative isothermal and kinetic study of the adsorption of lead (II) from solution by activated carbon and bentonite. *Journal of Engineering*, *21*(7), 45–58. https://doi.org/10.31026/j.eng.2015.07.04
2. Abdel Majeed, B. A., Muhseen, R. J., & Jassim, N. J. (2017). Adsorption of mefenamic acid from water by bentonite poly urea formaldehyde composite adsorbent. *Journal of Engineering*, *23*(7), 50–73. https://doi.org/10.31026/j.eng.2017.07.04
3. Abdel Moaty, S. A., Mahmoud, R. K., Mohamed, N. A., Gaber, Y., Farghali, A. A., Abdel Wahed, M. S. M., & Younes, H. A. (2019). Synthesis and characterisation of LDH-type anionic nanomaterials for the effective removal of doxycycline from aqueous media. *Water and Environment Journal*, wej.12526. https://doi.org/10.1111/wej.12526
4. Abed, M. F., & Faisal, A. A. H. (2023). Calcium/iron-layered double hydroxides-sodium alginate for removal of tetracycline antibiotic from aqueous solution. *Alexandria Engineering Journal*, *63*, 127–142. https://doi.org/10.1016/j.aej.2022.07.055
5. Ahmed, D.N., Naji, L. A., Faisal, A. A. H., Al-Ansari, N., & Naushad, M. (2020). Waste foundry sand/MgFe-layered double hydroxides composite material for efficient removal of Congo red dye from aqueous solution. *Scientific Reports*, *10*(1). https://doi.org/10.1038/s41598-020-58866-y
6. Ahmed, Dooraid N., Naji, L. A., Faisal, A. A. H., Al-Ansari, N., & Naushad, M. (2020). Waste foundry sand/MgFe-layered double hydroxides composite material for efficient removal of Congo red dye from aqueous solution. *Scientific Reports*, *10*(1), 2042. https://doi.org/10.1038/s41598-020-58866-y
7. Al-Kindi, G., & Alnasrawy, S. (2022). Tetracycline remove from synthetic wastewater by using several methods. *Journal of Ecological Engineering*, *23*(5), 137–148. https://doi.org/10.12911/22998993/146999
8. Alanazi, A. G., Habila, M. A., ALOthman, Z. A., & Badjah-Hadj-Ahmed, A.-Y. (2024). Synthesis and characterization of zinc oxide nanoparticle anchored carbon as hybrid adsorbent materials for effective heavy metals uptake from wastewater. *Crystals*, *14*(5), 447. https://doi.org/10.3390/cryst14050447
9. Asaoka, S., Kawakami, K., Saito, H., Ichinari, T., Nohara, H., & Oikawa, T. (2021). Adsorption of phosphate onto lanthanum-doped coal fly ash—Blast furnace cement composite. *Journal of Hazardous Materials*, *406*, 124780. https://doi.org/10.1016/j.jhazmat.2020.124780
10. Chen, B., Li, Y., Du, Q., Pi, X., Wang, Y., Sun, Y., … Zhu, J. (2022). Effective removal of tetracycline from water using copper alginate et graphene oxide with in-situ grown MOF-525 composite: Synthesis, characterization and adsorption mechanisms. *Nanomaterials*, *12*(17), 2897. https://doi.org/10.3390/nano12172897
11. Cheung, W. H., Szeto, Y. S., & McKay, G. (2007). Intraparticle diffusion processes during acid dye adsorption onto chitosan. *Bioresource Technology*, *98*(15), 2897–2904. https://doi.org/10.1016/j.biortech.2006.09.045
12. da Silva Bruckmann, F., Schnorr, C. E., da Rosa Salles, T., Nunes, F. B., Baumann, L., Müller, E. I., … Bohn Rhoden, C. R. (2022). Highly efficient adsorption of tetracycline using chitosan-based magnetic adsorbent. *Polymers*, *14*(22), 4854. https://doi.org/10.3390/polym14224854
13. Dai, Y., Liu, M., Li, J., Yang, S., Sun, Y., Sun, Q., … Liu, Z. (2020). A review on pollution situation and treatment methods of tetracycline in groundwater. *Separation Science and Technology*, *55*(5), 1005–1021. https://doi.org/10.1080/01496395.2019.1577445
14. Ebrahim, S. E., & Alhares, H. S. (2015). Competitive removal of Cu^{2+}, $Cd^{2+}$and Ni^{2+} by iron oxide nanoparticle (Fe_3O_4). *Journal of Engineering*, *21*(4), 98–122. https://doi.org/10.31026/j.eng.2015.04.06
15. Elkady, M. F., Mahmoud, M. M., & Abd-El-Rahman, H. M. (2011). Kinetic approach for cadmium sorption using microwave synthesized nano-hydroxyapatite. *Journal of Non-Crystalline Solids*, *357*(3), 1118–1129. https://doi.org/10.1016/j.jnoncrysol.2010.10.021
16. Elmoubarki, R., Mahjoubi, F. Z., Tounsadi, H., Moustadraf, J., Abdennouri, M., Zouhri, A., … Barka, N. (2015). Adsorption of textile dyes on raw and decanted Moroccan clays: Kinetics, equilibrium and thermodynamics. *Water Resources and Industry*, *9*, 16–29. https://doi.org/https://doi.org/10.1016/j.wri.2014.11.001
17. Faisal, A. A. H., Al-Ridah, Z. A., Naji, L. A., Naushad, M., & El-Serehy, H. A. (2020). Waste foundry sand as permeable and low permeable barrier for restriction of the propagation of lead and nickel ions in groundwater. *Journal of Chemistry*, *2020*, 1–13. https://doi.org/10.1155/2020/4569176
18. Ge, M., Du, M., Zheng, L., Wang, B., Zhou, X., Jia, Z., … Jahangir Alam, S. M. (2017). A maleic anhydride grafted sugarcane bagasse adsorbent and its performance on the removal of methylene blue from related wastewater. *Materials Chemistry and Physics*. https://doi.org/10.1016/j.matchemphys.2017.01.063
19. Greenwell, H. C., Jones, W., Rugen-Hankey, S. L., Holliman, P. J., & Thompson, R. L. (2010). Efficient synthesis of ordered organo-layered double hydroxides. *Green Chemistry*, *12*(4), 688. https://doi.org/10.1039/b916301h

20. Islam, M., Ahmed, N., Hossain, M., Rahman, A., & Sultana, A. (2016). Effect of pH on the adsorption kinetics of Cr(VI) on sodium chlorite treated coconut coir. *Bangladesh Journal of Scientific and Industrial Research*, *51*(2), 95–100. https://doi.org/10.3329/bjsir.v51i2.28090
21. Kameliya, J., Verma, A., Dutta, P., Arora, C., Vyas, S., & Varma, R. S. (2023). Layered double hydroxide materials: A review on their preparation, characterization, and applications. *Inorganics*, *11*(3), 121. https://doi.org/10.3390/inorganics11030121
22. Kiani, M., Bagherzadeh, M., Ghadiri, A. M., Makvandi, P., & Rabiee, N. (2022). Multifunctional green synthesized Cu–Al layered double hydroxide (LDH) nanoparticles: anti-cancer and antibacterial activities. *Scientific Reports*, *12*(1), 9461. https://doi.org/10.1038/s41598-022-13431-7
23. Lucas, S., Cocero, M. J., Zetzl, C., & Brunner, G. (2004). Adsorption isotherms for ethylacetate and furfural on activated carbon from supercritical carbon dioxide. *Fluid Phase Equilibria*. https://doi.org/10.1016/j.fluid.2004.01.034
24. Luo, H., Liu, Y., Lu, H., Fang, Q., & Rong, H. (2021). Efficient adsorption of tetracycline from aqueous solutions by modified alginate beads after the removal of Cu(II) Ions. *ACS Omega*, *6*(9), 6240–6251. https://doi.org/10.1021/acsomega.0c05807
25. McKay, G., Porter, J. F., & Prasad, G. R. (1999). The removal of dye colours from aqueous solutions by adsorption on low- cost materials. *Water, Air, and Soil Pollution*. https://doi.org/10.1023/A:1005197308228
26. Osman, A. I., Zhang, Y., Farghali, M., Rashwan, A. K., Eltaweil, A. S., Abd El-Monaem, E. M., … Yap, P.-S. (2024). Synthesis of green nanoparticles for energy, biomedical, environmental, agricultural, and food applications: A review. *Environmental Chemistry Letters*, *22*(2), 841–887. https://doi.org/10.1007/s10311-023-01682-3
27. Park, J. B., Lee, S. H., Lee, J. W., & Lee, C. Y. (2002). Lab scale experiments for permeable reactive barriers against contaminated groundwater with ammonium and heavy metals using clinoptilolite (01-29B). *Journal of Hazardous Materials*. https://doi.org/10.1016/S0304-3894(02)00007-9
28. Qiu, H., Lv, L., Pan, B., Zhang, Q., Zhang, W., & Zhang, Q. (2009). Critical review in adsorption kinetic models. *Journal of Zhejiang University-SCIENCE A*, *10*(5), 716–724. https://doi.org/10.1631/jzus.A0820524
29. Rashid, M. H., & Faisal, A. H. A. (2018). Removal of dissolved cadmium ions from contaminated wastewater using raw scrap zero-valent iron and zero valent aluminum as locally available and inexpensive sorbent wastes. *Iraqi Journal of Chemical and Petroleum Engineering*, *19*(4), 39–45. https://doi.org/10.31699/ijcpe.2018.4.5
30. Sadegh, H., Ali, G. A. M., Gupta, V. K., Makhlouf, A. S. H., Shahryari-ghoshekandi, R., Nadagouda, M. N., … Megiel, E. (2017). The role of nanomaterials as effective adsorbents and their applications in wastewater treatment. *Journal of Nanostructure in Chemistry*, *7*(1), 1–14. https://doi.org/10.1007/s40097-017-0219-4
31. Salman, M. S., Abood, W. M., & Ali, D. (2023). Batch and fixed-bed modeling of adsorption reactive remazol yellow dye onto granular activated carbon. *Journal of Engineering*, *20*(08), 156–176. https://doi.org/10.31026/j.eng.2014.08.10
32. Singha Roy, A., Kesavan Pillai, S., & Ray, S. S. (2022). Layered double hydroxides for sustainable agriculture and environment: An overview. *ACS Omega*, *7*(24), 20428–20440. https://doi.org/10.1021/acsomega.2c01405
33. Sutherland, R. A., & Tack, F. M. G. (2008). Extraction of labile metals from solid media by dilute hydrochloric acid. *Environmental Monitoring and Assessment*, *138*(1–3), 119–130. https://doi.org/10.1007/s10661-007-9748-5
34. Tonelli, D., Gualandi, I., Musella, E., & Scavetta, E. (2021). Synthesis and characterization of layered double hydroxides as materials for electrocatalytic applications. *Nanomaterials*, *11*(3), 725. https://doi.org/10.3390/nano11030725
35. Ujaczki, É., Zimmermann, Y. S., Gasser, C. A., Molnár, M., Feigl, V., & Lenz, M. (2017). Red mud as secondary source for critical raw materials – extraction study. *Journal of Chemical Technology & Biotechnology*, *92*(11), 2835–2844. https://doi.org/10.1002/jctb.5300
36. Wang, K., Yao, R., Zhang, D., Peng, N., Zhao, P., Zhong, Y., … Liu, C. (2023). Tetracycline adsorption performance and mechanism using calcium hydroxide-modified biochars. *Toxics*, *11*(10), 841. https://doi.org/10.3390/toxics11100841
37. Wang, S., & Wang, H. (2015). Adsorption behavior of antibiotic in soil environment: a critical review. *Frontiers of Environmental Science & Engineering*, *9*(4), 565–574. https://doi.org/10.1007/s11783-015-0801-2
38. Yagub, M. T., Sen, T. K., & Ang, H. M. (2012). Equilibrium, kinetics, and thermodynamics of methylene blue adsorption by pine tree leaves. *Water, Air, and Soil Pollution*, Vol. 223, pp. 5267–5282. https://doi.org/10.1007/s11270-012-1277-3
39. Yaseen, R. A. A., Ibrahim, M. A., & Ahmed, M. (2022). The effect of Schanginia aegyptica and Urtica dioica powder on the growth of Trigonella foenum seedlings in laboratory sterilized soil. *HIV Nursing*, *22*, 243–247.
40. Zhang, P., Liu, C., Lao, D., Nguyen, X. C., Paramasivan, B., Qian, X., … Li, F. (2023). Unveiling the drives behind tetracycline adsorption capacity with biochar through machine learning. *Scientific Reports*, *13*(1), 11512. https://doi.org/10.1038/s41598-023-38579-8